Multiwavelength Observations of the VHE Blazar 1ES 2344+514

V. A. Acciari[1], E. Aliu[2], T. Arlen[3], T. Aune[4], M. Beilicke[5], W. Benbow[1], D. Boltuch[2], V. Bugaev[5], A. Cannon[6], L. Ciupik[7], P. Cogan[8], P. Colin[9], R. Dickherber[5], A. Falcone[10], S. J. Fegan[3], J. P. Finley[11], P. Fortin[12], L. F. Fortson[7], A. Furniss[4], D. Gall[11], G. H. Gillanders[13], J. Grube[6,7,*] R. Guenette[8], G. Gyuk[7], D. Hanna[8], J. Holder[2], D. Horan[14], C. M. Hui[9], T. B. Humensky[15], A. Imran[16], P. Kaaret[17], N. Karlsson[7], M. Kertzman[18], D. Kieda[9], J. Kildea[1], A. Konopelko[19], H. Krawczynski[5], F. Krennrich[16], M. J. Lang[13], S. LeBohec[9], G. Maier[8], P. Moriarty[20], R. Mukherjee[12], R. A. Ong[3], A. N. Otte[4], D. Pandel[17], J. S. Perkins[1], A. Pichel[21], M. Pohl[16], J. Quinn[6], K. Ragan[8], P. T. Reynolds[22], H. J. Rose[23], M. Schroedter[16], G. H. Sembroski[11], A. W. Smith[24], D. Steele[7], S. P. Swordy[15], M. Theiling[1], J. A. Toner[13], A. Varlotta[11], V. V. Vassiliev[3], S. Vincent[9], R. Wagner[24], S. P. Wakely[15], J. E. Ward[6], T. C. Weekes[1], A. Weinstein[3], T. Weisgarber[15], D. A. Williams[4], S. Wissel[15], M. Wood[3], B. Zitzer[11]

ABSTRACT

Multiwavelength observations of the high-frequency-peaked blazar 1ES 2344+514 were performed from 2007 October to 2008 January. The campaign represents the first contemporaneous data on the object at very high energy (VHE, E >100 GeV) γ-ray, X-ray, and UV energies. Observations with VERITAS in VHE γ-rays yield a strong detection of 20 σ with 633 excess events in a total exposure of 18.1 hours live-time. A strong VHE γ-ray flare on 2007 December 7 is measured at F(>300 GeV) = $(6.76 \pm 0.62) \times 10^{-11}$ ph cm^{-2} s^{-1}, corresponding to 48% of the Crab Nebula flux. Excluding this flaring episode, nightly variability at lower fluxes is observed with a time-averaged mean of F(>300 GeV) = $(1.06 \pm 0.09) \times 10^{-11}$ ph cm^{-2} s^{-1} (7.6% of the Crab Nebula flux). The differential photon spectrum between 390 GeV and 8.3 TeV for the time-averaged observations excluding 2007 December 7 is well described by a power law with a photon index of $\Gamma = 2.78 \pm 0.09_{\rm stat} \pm 0.15_{\rm syst}$. On the flaring night of 2007 December 7 the measured VHE γ-ray photon index was $\Gamma = 2.43 \pm 0.22_{\rm stat} \pm 0.15_{\rm syst}$. Over the full period of VERITAS observations contemporaneous X-ray and UV data were taken with *Swift* and *RXTE*. The measured 2–10 keV flux ranged by a factor of $\sim$7 during the campaign. On 2007 December 8 the highest ever observed X-ray flux from 1ES 2344+514 was measured by *Swift* XRT at a flux of F(2–10 keV) = $(6.28 \pm 0.31) \times 10^{-11}$ erg cm^{-2} s^{-1}. Evidence for a correlation between the X-ray flux and VHE γ-ray flux on nightly time-scales is indicated with a Pearson correlation coefficient of $r = 0.60 \pm 0.11$. Contemporaneous spectral energy distributions (SEDs) of 1ES 2344+514 are presented for two distinct flux states. A one-zone synchrotron self-Compton (SSC) model describes both SEDs using parameters consistent with previous SSC modeling of 1ES 2344+514 from non-contemporaneous observations.

Subject headings: galaxies: BL Lacertae objects: individual: 1ES 2344+514

[1]Fred Lawrence Whipple Observatory, Harvard-Smithsonian Center for Astrophysics, Amado, AZ 85645, USA

[2]Department of Physics and Astronomy and the Bartol Research Institute, University of Delaware, Newark, DE 19716, USA

[3]Department of Physics and Astronomy, University of

1. Introduction

The majority of blazars detected at very high energy (VHE, E >100 GeV) γ-rays are high-frequency-peaked BL Lac objects (HBLs), with currently ~25 HBLs from a total of ~30 VHE blazars.[1] The short time-scale variability seen in the broadband spectral energy distributions (SEDs) of blazars is explained by highly relativistic plasma jets oriented close to the line of sight (Blandford & Königl 1979). HBLs are blazars exhibiting synchrotron radiation peaking typically at UV to X-ray energies and a second SED component peaking at GeV to TeV energies. Leptonic models (Coppi 1992; Böttcher & Chang 2002; Krawczynski et al. 2004) describe the high-energy peak as inverse Compton upscattering of low-energy photons by electrons, while hadronic models attribute the emission to proton-induced cascades, synchrotron radiation by protons, pion production in dense clumps of jet plasma, or curvature radiation (Mannheim 1993; Aharonian 2000; Mücke & Protheroe 2001). Detailed multi-wavelength studies from optical to γ-ray energies of the temporal and spectral variability of HBLs promise to constrain the physical parameters of the underlying particle distributions, particularly the Doppler factor and magnetic field strength (Tavecchio, Maraschi & Ghisellini 1998).

The HBL 1ES 2344+514 was first detected in the Einstein Slew Survey at X-ray energies (0.2–4 keV) and has a redshift of z = 0.044 (Elvis et al. 1992; Perlman et al. 1996). VHE γ-ray emission from 1ES 2344+514 was discovered by the Whipple 10 m telescope in energies >350 GeV at a 6.0 σ detection level during a 1 day flare on 1995 December 20 (Catanese et al. 1998). X-ray observations of 1ES 2344+514 with *BeppoSAX* revealed variability in the 2–10 keV flux by a factor of ~2 during a 7-day period in 1996 December (Giommi et al. 2000). 1ES 2344+514 was later observed by *Swift* in 2005 during April, May, and December at a lower flux than in 1996 December (Tramacere et al. 2007). The X-ray spectrum is reasonably well described by an absorbed power law, with photon indices ranging from $\Gamma \approx 1.8$–2.3. Marginal evidence for optical variability in 1ES 2344+514 is seen from the sparse data set of two observations in 1998 (Nilsson et al. 1999; Falomo & Kotilainen 1999), six nights in 2000 (Xie et al. 2002), and one observation on 2007 January 12 (Gupta et al. 2008). In the radio band, VLA observations reveal an unusual morphology

California, Los Angeles, CA 90095, USA

[4]Santa Cruz Institute for Particle Physics and Department of Physics, University of California, Santa Cruz, CA 95064, USA

[5]Department of Physics, Washington University, St. Louis, MO 63130, USA

[6]School of Physics, University College Dublin, Belfield, Dublin 4, Ireland

[7]Astronomy Department, Adler Planetarium and Astronomy Museum, Chicago, IL 60605, USA

[8]Physics Department, McGill University, Montreal, QC H3A 2T8, Canada

[9]Physics Department, University of Utah, Salt Lake City, UT 84112, USA

[10]Department of Astronomy and Astrophysics, 525 Davey Lab, Pennsylvania State University, University Park, PA 16802, USA

[11]Department of Physics, Purdue University, West Lafayette, IN 47907, USA

[12]Department of Physics and Astronomy, Barnard College, Columbia University, NY 10027, USA

[13]School of Physics, National University of Ireland, Galway, Ireland

[14]Laboratoire Leprince-Ringuet, Ecole Polytechnique, CNRS/IN2P3, F-91128 Palaiseau, France

[15]Enrico Fermi Institute, University of Chicago, Chicago, IL 60637, USA

[16]Department of Physics and Astronomy, Iowa State University, Ames, IA 50011, USA

[17]Department of Physics and Astronomy, University of Iowa, Van Allen Hall, Iowa City, IA 52242, USA

[18]Department of Physics and Astronomy, DePauw University, Greencastle, IN 46135-0037, USA

[19]Department of Physics, Pittsburg State University, 1701 South Broadway, Pittsburg, KS 66762, USA

[20]Department of Life and Physical Sciences, Galway-Mayo Institute of Technology, Dublin Road, Galway, Ireland

[21]Instituto de Astronomia y Fisica del Espacio, Casilla de Correo 67 - Sucursal 28, (C1428ZAA) Ciudad Autnoma de Buenos Aires, Argentina

[22]Department of Applied Physics and Instrumentation, Cork Institute of Technology, Bishopstown, Cork, Ireland

[23]School of Physics and Astronomy, University of Leeds, Leeds, LS2 9JT, UK

[24]Argonne National Laboratory, 9700 S. Cass Avenue, Argonne, IL 60439, USA

[*]Corresponding author: jgrube@adlerplanetarium.org

[1]The TeVCat catalog of VHE γ-rays sources is available online at: http://tevcat.uchicago.edu

at arcsec scales for a blazar of two compact high brightness emission regions connected via a diffuse halo, more reminiscent of a radio galaxy (Rector, Gabuzda & Stocke 2003; Giroletti et al. 2004). High resolution VLBA observations show a well-collimated jet extending ∼10 pc from the core, which then bends 25° and broadens into a cone of ∼35° opening angle. In high energy (HE, 0.1>E<300 GeV) γ-rays, 1ES 2344+514 is associated with the source 1FGL J2347.1+5142 from the *Fermi* LAT First Source Catalog (Abdo et al. 2010), detected at a significance of 10.6 σ and showing a hard HE γ-ray spectrum of 1.57 ± 0.17 with no indication of HE γ-ray flux variability during the period of 2008 August to 2009 July.

Evidence for long-term VHE γ-ray flux variability in 1ES 2344+514 is seen in observations between 1995 and 2005 by the Whipple 10 m telescope, HEGRA, and MAGIC. The Whipple 10 m γ-ray photon spectrum on the flaring night of 1995 December 20 is best-fit by a power law over the energy range 0.8–9 TeV, with a photon index $\Gamma = 2.54 \pm 0.17_{\rm stat} \pm 0.07_{\rm syst}$ (Schroedter et al. 2005). The measured flux F(>1 TeV) = $(3.3 \pm 0.7) \times 10^{-11}$) ph cm^{-2} s^{-1} for the flare night is a factor of 1.7 ± 0.3 higher than the Crab Nebula flux. Excluding 1995 December 20, the time-averaged Whipple 10 m data between 1995 and 1997 yielded a marginal 4 σ detection at a significantly lower flux level, corresponding to ∼10% of the Crab Nebula flux (Catanese et al. 1998). Further VHE γ-ray observations of 1ES 2344+514 with HEGRA in 1997, 1998, and 2002 resulted in a 4.4 σ detection in a low flux level state of (3.3 ± 1.0)% of the Crab Nebula flux (Aharonian et al. 2004). Observations in 1995 with TACTIC above 1.5 TeV in 2004 and 2005 yielded a weakly constraining flux upper limit near the Whipple 10 m detection flux level (Godambe et al. 2007). In 2005 August to 2006 January, the MAGIC telescope measured a time-averaged photon spectrum between 0.14–5.4 TeV at a low flux of 5% of the Crab Nebula flux characterized by a power-law with $\Gamma = 2.95 \pm 0.12_{\rm stat} \pm 0.20_{\rm syst}$ (Albert et al. 2007). This article presents the first multiwavelength campaign on 1ES 2344+514, with contemporaneous UV, X-ray and VHE γ-ray observations over a several month long period.

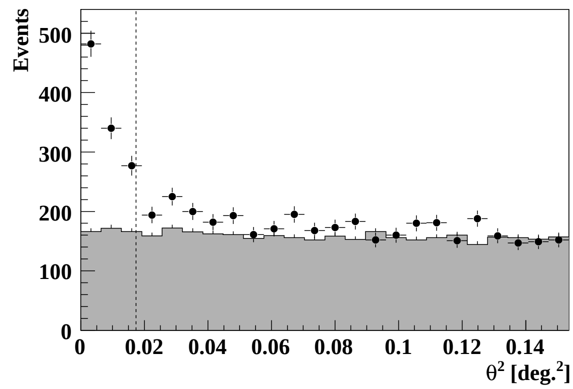

Fig. 1.— The distribution of θ^2 for on-source events (points) and normalized off-source events (shaded region) from observations of 1ES 2344+514. The dashed line represents the applied cut on the θ^2 parameter.

2. VERITAS Observations

VERITAS is an array of four 12 m diameter imaging atmospheric Cherenkov telescopes located at the Fred Lawrence Whipple Observatory in Southern Arizona (Weekes et al. 2002). Each VERITAS camera contains 499 pixels (0.15° diameter), and has a field of view of 3.5°. VERITAS is sensitive over an energy range of ∼100 GeV to ∼30 TeV with an energy resolution of 15–20%, and an angular resolution (68% containment) of less than 0.14° per event (Acciari et al. 2008). VERITAS can detect VHE γ-ray fluxes of 5% and 1% of the Crab Nebula flux at the 5 σ level in <2.5 and <50 hours, respectively.

The VERITAS observations of 1ES 2344+514 presented here were taken on 37 nights between 2007 October 4 and 2008 January 11. After applying quality-selection criteria, the total exposure is 18.1 hours live-time. Data-quality selection requires clear atmospheric conditions, based on infrared sky temperature measurements, and normal hardware operation. During each night, the quality-selected data ranged from 0.3–2.7 hours live-time. The zenith angle of observations ranges from 19–48°, with a mean of 28°. All data were taken during moon-less periods in *wobble* mode with pointings of 0.5° from the blazar alternating from North, South, East, and West directions to enable simultaneous background estimation (Aharonian et al. 2001).

Data reduction followed the methods described in Acciari et al. (2008). Signals in each event are first calibrated (Holder et al. 2006), and the images are parameterized (Hillas 1985). The γ-ray direction and air shower impact parameter on the ground are then reconstructed using stereoscopic techniques (Hofmann et al. 1999; Krawczynski et al. 2006). The background of cosmic-rays is rejected with a very high efficiency using event-by-event cuts on the arrival direction (θ^2), mean scaled width and length, integrated charge (*size*), and location of the image centroids in the camera (*distance*). The cuts applied here are optimized *a priori* for a source strength of 10% of the Crab Nebula flux and a similar photon index to the Crab Nebula. The energy of each event is reconstructed using lookup tables from Monte Carlo simulations of γ-rays (Acciari et al. 2008). Results from two independent VERITAS analysis packages (Daniel et al. 2007) yield results consistent with those presented here.

A total of 1275 on-source and 4494 off-source events were measured, with an on-off normalization of $\alpha = 0.143$. This corresponds to a total excess of 632 events from the direction of 1ES 2344+514. The statistical significance of this excess is 20.2 standard deviations (σ). Figure 1 shows the θ^2 distribution of the total data set, which is the squared angular distance between the reconstructed event direction and the nominal source position. The shape of the excess is consistent with a simulated point source for VERITAS.

3. *RXTE* Observations

The X-ray satellite mission *RXTE* (Bradt et al. 1993) observed 1ES 2344+514 between 2007 October 7 and 2008 January 11 (ObsID 93132). Data are presented from Proportional Counter Unit 2 of the PCA instrument (Jahoda et al. 1996) since for nearly all observations the other PCUs were not in operation. The 52 nightly PCA observations were taken in snapshots ranging from 0.11-1.00 hours live-time, and are listed in Table 1. Data reduction is performed with the *HEAsoft* 6.5 package. Only the top layer (X1L and X1R) signal is used. The data are filtered following the standard criteria advised by the NASA Guest Observer Facility. Background data are parameterized with the *pcabackest* tool using the most recent model for faint sources. The photon spectrum of each observation is extracted using the *saextrct* tool. Response matrices are generated using *pcarsp* with the latest calibration files.

4. *Swift* Observations

Swift (Gehrels et al. 2004) Target of Opportunity (ToO) observations of 1ES 2344+514 from 2007 October 27 to 2008 January 1 were triggered by the VERITAS detection. The *Swift* data set consists of eight snapshot observations of 10–45 minute duration each, as listed in Table 1. All *Swift* XRT data (Burrows et al. 2005) are reduced using the *HEAsoft* 6.5 package. Event files are calibrated and cleaned following the standard filtering criteria using the *xrtpipeline* task and applying the most recent *Swift* XRT calibration files. All data were taken in Photon Counting (PC) mode, with grades 0–12 selected over the energy range 0.3–10 keV. Due to photon pile-up in the core of the point spread function (PSF) at count rates >0.5 counts s^{-1} (PC mode), the source events are extracted from an annular region with inner radius ranging from 2–6 pixels and an outer radius of 30 pixels (47.2 arcsec). Background counts are extracted from a 40 pixel radius circle in a source-free region. Ancillary response files are generated using the *xrtmkarf* task, with corrections applied for the PSF losses and CCD defects. The latest response matrix from the XRT calibration files is applied. To ensure valid χ^2 minimization statistics during spectral fitting, the extracted XRT energy spectra are rebinned to contain a minimum of 30 counts in each bin.

UVOT observations were taken in the photometric bands of *UVW1*, *UVM2*, and *UVW2* (Poole et al. 2008). The *uvotsource* tool is used to extract counts, correct for coincidence losses, apply background subtraction, and calculate the source flux. The standard 5 arcsec radius source aperture is used, with a 20 arcsec background region. The source fluxes are dereddened using the interstellar extinction curve in Fitzpatrick (1999). In the UV filters only a low level of host galaxy flux is evident (Tramacere et al. 2007), so no corrections are needed. The uncertainty in point spread function variations with time is fixed for this analysis at 15%. Observations were taken with just one

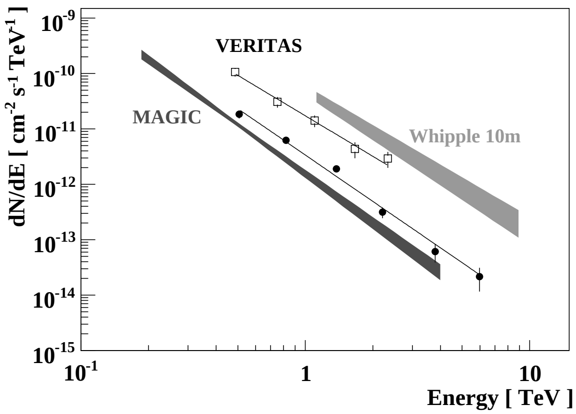

Fig. 2.— Differential photon spectrum of VHE γ-rays for 1ES 2344+514. The circles represent the time-averaged VERITAS data from 2007 October to 2008 January, excluding the bright flare on 2007 December 7. The open squares represent VERITAS data from the flare night. Shown for comparison are the 68% confidence intervals for the best-fit power law models to 1ES 2344+514 data from MAGIC (dark grey band) in 2005 August to 2006 January (Albert et al. 2007), and from the Whipple 10 m (light grey band) during a high flux state on 1995 December 20 (Schroedter et al. 2005).

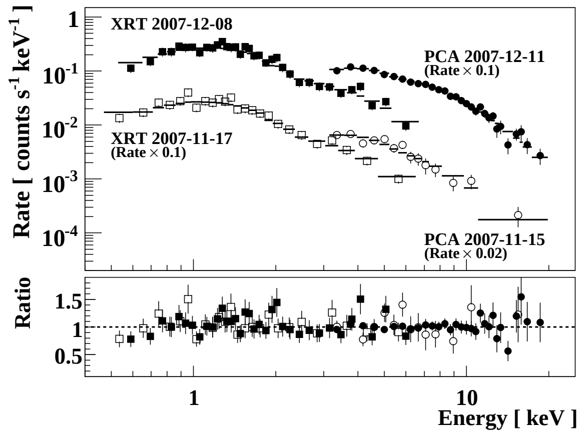

Fig. 3.— X-ray spectrum of 1ES 2344+514 from *Swift* XRT and *RXTE* PCA observations. Shown in the top panel are example moderate-flux and high-flux spectra identified in the plot by instrument and observation date. The differential rates are scaled in three cases for viewing purposes. For each energy bin, the statistical significance is $>3\,\sigma$, and the horizontal line represents the best-fit forward folded absorbed power law model. The bottom panel shows the ratio of the data and model values.

UV filter during each pointing, and only *UVM2* data were taken on multiple nights. Within the conservative errors, no variability is seen between the four *UVM2* filter observations.

5. Spectral Analysis

The VERITAS differential photon spectrum over the energy range of 390 GeV to 8.3 TeV for the time-averaged data excluding a strong flaring night on 2007 December 7 is shown in Figure 2. A power law model fit to the data is best described by the form $d\mathrm{N}/\mathrm{dE} = \mathrm{F}_\circ \cdot (\mathrm{E}/1\mathrm{TeV})^{-\Gamma}$ yielding a χ^2/dof of 8.39/4 for a flux normalization constant of $\mathrm{F}_\circ = (3.38 \pm 0.23_{\mathrm{stat}} \pm 0.70_{\mathrm{syst}}) \times 10^{-12}$ ph cm^{-2} s^{-1} TeV^{-1} and a photon index of $\Gamma = 2.78 \pm 0.09_{\mathrm{stat}} \pm 0.15_{\mathrm{syst}}$. A fit to a power law with exponential cutoff model, which contains one additional degree of freedom, does not yield a significantly better fit. On 2007 December 7 the weather conditions were affected by moving cloud coverage, so the observations do not pass the standard data-quality criteria. However, online analysis showed that the source was in the most active state yet observed. We therefore include these data and increase the systematic uncertainties in flux and spectral shape. Conservative systematic uncertainties in the flux of 30% and photon index of 0.2 are determined, based on the results of observations of the Crab Nebula taken in similarly variable conditions. The VHE γ-ray spectrum from the high flux night is well described by a power law (χ^2/dof of 1.27/3) with a slightly harder photon index $\Gamma = 2.43 \pm 0.22_{\mathrm{stat}} \pm 0.2_{\mathrm{syst}}$, and a higher flux normalization of $\mathrm{F}_\circ = (17.3 \pm 1.92_{\mathrm{stat}} \pm 5.19_{\mathrm{syst}}) \times 10^{-12}$ ph cm^{-2} s^{-1} TeV^{-1}.

The best-fit results presented here are tested with a dedicated Monte-Carlo study, which explores the uncertainty ranges for the two measured spectra. In the Monte-Carlo study photons are selected from a power-law distribution matching the measured distribution convolved with the effective area as a function of energy. The selected photon energies are then smeared with a Gaussian corresponding to the energy resolution of $\sim$15% at these energies. The number of photons selected is

Table 1: Best-fit spectral parameters for the *Swift* XRT and *RXTE* PCA data.

Date	Start (hr:min UT)	Exp. (ksec)	Γ	K_{1keV} (10^{-2} ph cm^{-2} s^{-1} keV^{-1})	χ^2_r/dof	F(2–10 keV) (10^{-11} erg cm^{-2} s^{-1})
Swift XRT						
2007-10-27	10:24	2.66	2.33 ± 0.05	0.62 ± 0.03	1.11/36	0.96 ± 0.06
2007-11-03	03:02	1.97	2.32 ± 0.06	0.87 ± 0.04	1.02/27	1.37 ± 0.09
2007-11-10	05:03	0.63	2.26 ± 0.13	1.26 ± 0.10	0.69/8	2.18 ± 0.31
2007-11-17	02:28	1.65	2.16 ± 0.06	0.76 ± 0.04	0.71/23	1.51 ± 0.14
2007-11-30	03:46	1.85	2.10 ± 0.07	0.91 ± 0.05	1.51/23	1.99 ± 0.14
2007-12-08	03:20	2.22	1.97 ± 0.05	2.37 ± 0.10	0.77/33	6.28 ± 0.31
2007-12-22	04:28	2.23	2.18 ± 0.05	1.00 ± 0.04	1.12/36	1.93 ± 0.13
2008-01-01	00:35	1.37	2.10 ± 0.08	1.26 ± 0.07	1.07/18	2.72 ± 0.17
RXTE PCA						
2007-10-07	06:03	2.56	2.48 ± 0.26	0.75 ± 0.35	0.52/38	0.95 ± 0.26
2007-10-08	06:56	2.88	2.65 ± 0.20	1.24 ± 0.38	0.58/38	1.24 ± 0.15
2007-10-09	06:14	2.80	2.31 ± 0.13	1.04 ± 0.23	0.54/38	1.66 ± 0.10
2007-10-10	05:53	2.67	2.17 ± 0.12	0.89 ± 0.19	0.47/38	1.76 ± 0.14
2007-10-11	03:42	2.16	2.57 ± 0.15	1.65 ± 0.40	0.42/38	1.85 ± 0.11
2007-10-12	03:14	0.21	2.57 ± 0.19	1.34 ± 0.41	0.66/38	1.48 ± 0.15
2007-10-13	04:52	2.02	2.26 ± 0.13	1.11 ± 0.24	0.63/38	1.92 ± 0.15
2007-10-14	02:17	1.86	2.39 ± 0.12	1.63 ± 0.33	0.62/38	2.35 ± 0.14
2007-10-15	03:56	1.50	2.49 ± 0.16	1.61 ± 0.41	0.53/38	2.02 ± 0.20
2007-10-16	04:35	1.84	2.25 ± 0.18	0.80 ± 0.27	0.53/38	1.41 ± 0.24
2007-10-19	07:09	3.62	2.42 ± 0.14	1.02 ± 0.23	0.51/38	1.39 ± 0.13
2007-10-20	08:18	3.15	2.61 ± 0.15	1.51 ± 0.35	0.59/38	1.59 ± 0.12
2007-10-21	07:57	3.49	2.36 ± 0.16	0.81 ± 0.23	0.56/38	1.22 ± 0.11
2007-11-01	03:06	2.59	2.19 ± 0.15	0.73 ± 0.21	0.79/38	1.40 ± 0.13
2007-11-02	05:53	1.39	2.41 ± 0.18	1.25 ± 0.37	0.62/38	1.73 ± 0.16
2007-11-03	07:06	2.37	2.72 ± 0.19	1.65 ± 0.48	0.53/38	1.50 ± 0.14
2007-11-04	04:56	2.85	2.19 ± 0.14	0.75 ± 0.20	0.50/38	1.43 ± 0.11
2007-11-05	06:35	0.80	2.20 ± 0.29	0.68 ± 0.40	0.64/38	1.28 ± 0.45
2007-11-06	04:02	2.48	2.23 ± 0.11	1.10 ± 0.21	0.82/38	2.00 ± 0.11
2007-11-07	06:36	0.31	2.43 ± 0.12	1.28 ± 0.25	0.49/38	1.75 ± 0.09
2007-11-08	07:52	2.96	2.20 ± 0.10	1.10 ± 0.18	0.57/38	2.07 ± 0.11
2007-11-09	07:35	2.40	2.10 ± 0.09	1.16 ± 0.17	0.59/38	2.53 ± 0.12
2007-11-10	03:50	2.53	2.13 ± 0.08	1.41 ± 0.18	0.33/38	2.94 ± 0.09
2007-11-11	01:49	2.27	2.16 ± 0.08	1.50 ± 0.20	0.63/38	3.02 ± 0.13
2007-11-12	04:31	2.51	2.23 ± 0.13	0.91 ± 0.21	0.54/38	1.65 ± 0.16
2007-11-13	02:30	2.30	2.11 ± 0.09	1.19 ± 0.18	0.71/38	2.57 ± 0.13
2007-11-14	03:37	2.40	2.22 ± 0.11	1.15 ± 0.21	0.55/38	2.12 ± 0.10
2007-11-15	03:10	2.34	2.50 ± 0.16	1.31 ± 0.33	0.60/38	1.61 ± 0.15
2007-11-30	02:20	0.37	2.44 ± 0.26	1.91 ± 0.81	0.74/38	2.54 ± 0.37
2007-12-01	01:51	0.50	2.59 ± 0.33	1.62 ± 0.84	0.38/38	1.76 ± 0.46
2007-12-02	05:03	0.58	2.23 ± 0.18	1.48 ± 0.43	0.72/38	2.65 ± 0.25
2007-12-04	02:31	0.40	2.10 ± 0.19	1.32 ± 0.42	0.61/38	2.87 ± 0.39
2007-12-05	02:11	1.79	2.01 ± 0.05	2.15 ± 0.19	0.81/38	5.37 ± 0.15
2007-12-06	03:28	1.57	2.06 ± 0.06	1.99 ± 0.22	0.69/38	4.63 ± 0.11
2007-12-10	02:18	2.03	1.94 ± 0.06	1.39 ± 0.15	0.90/38	3.90 ± 0.10
2007-12-11	02:50	1.82	1.87 ± 0.04	1.97 ± 0.15	0.62/38	6.10 ± 0.11
2007-12-13	03:38	3.39	1.86 ± 0.04	1.54 ± 0.10	0.67/38	4.85 ± 0.07
2007-12-12	05:41	1.23	1.97 ± 0.06	1.96 ± 0.21	0.46/38	5.20 ± 0.13
2007-12-14	04:35	3.33	2.08 ± 0.06	1.53 ± 0.15	0.65/38	3.42 ± 0.09
2007-12-15	04:53	0.86	2.17 ± 0.13	1.57 ± 0.33	0.91/38	3.10 ± 0.23
2007-12-28	03:46	1.06	2.14 ± 0.11	1.48 ± 0.28	0.72/38	3.06 ± 0.17
2007-12-29	04:53	1.17	1.96 ± 0.15	0.69 ± 0.22	0.47/38	1.86 ± 0.23
2007-12-30	04:25	0.88	1.91 ± 0.09	1.40 ± 0.22	0.56/38	4.04 ± 0.22
2008-01-01	01:52	0.86	2.06 ± 0.11	1.43 ± 0.27	0.85/38	3.30 ± 0.15
2008-01-02	02:26	2.66	2.12 ± 0.07	1.40 ± 0.17	0.53/38	2.96 ± 0.11
2008-01-03	03:34	2.91	1.97 ± 0.06	1.23 ± 0.13	0.67/38	3.26 ± 0.10
2008-01-04	01:53	1.71	2.06 ± 0.13	0.87 ± 0.20	0.65/38	2.03 ± 0.12
2008-01-05	02:35	2.83	1.97 ± 0.07	1.02 ± 0.13	0.51/38	2.71 ± 0.11
2008-01-06	02:08	2.75	2.31 ± 0.12	1.08 ± 0.22	0.41/38	1.76 ± 0.11
2008-01-07	03:48	1.98	2.33 ± 0.14	1.16 ± 0.27	0.68/38	1.83 ± 0.12
2008-01-10	02:23	1.50	2.25 ± 0.10	1.78 ± 0.29	0.52/38	3.12 ± 0.14
2008-01-11	03:24	2.77	2.12 ± 0.07	1.53 ± 0.17	0.74/38	3.25 ± 0.10

matched to the observed number of photons with a Poisson scatter. Five million synthetic photon spectra are created using similar binning to the original spectra, and the best-fit power law index and normalization parameters are extracted for each synthetic spectrum providing dense coverage of the parameter space. The Monte-Carlo mean value and one dimensional standard deviation of the power law parameters are consistent with the best-fit parameters of the measured spectra. For the time-averaged spectrum excluding the flaring night of 2007 December 7, the Monte-Carlo study yields a mean value and 1-σ error for the flux normalization of $F_{\circ,MC} = (3.35 \pm 0.30) \times 10^{-12}$ ph cm^{-2} s^{-1} TeV^{-1} and for the the photon index of $\Gamma_{MC} = 2.76 \pm 0.15$. For the high flux 2007 December 7 spectrum, the Monte-Carlo study yields $F_{\circ,MC} = (17.3 \pm 2.67) \times 10^{-12}$ ph cm^{-2} s^{-1} TeV^{-1} and $\Gamma_{MC} = 2.40 \pm 0.28$.

Previous VHE γ-ray observations of 1ES 2344+514 with the MAGIC telescope between 2005 August and 2006 January measured a constant flux at a slightly lower level than the time-averaged (flare excluded) flux measured here, and a consistent photon index of $\Gamma = 2.95 \pm 0.12_{\rm stat.} \pm 0.2_{\rm syst.}$ (Albert et al. 2007). The high flux VHE γ-ray photon spectrum measured by the Whipple 10 m on 1995 December 20 with a photon index of $\Gamma = 2.54 \pm 0.17_{\rm stat} \pm 0.07_{\rm syst}$ (Schroedter et al. 2005) is marginally harder than the low flux spectrum and agrees with the high flux spectrum measured here. The VHE observed γ-ray spectral shape and intensity are modified by absorption from pair production interactions with the infrared component of the extragalactic background light (EBL) (Gould & Schréder 1967). Using the redshift z = 0.044 for 1ES 2344+514, we calculate a de-absorbed spectrum based on the EBL model of Franceschini et al. (2008), yielding intrinsic photon indices for the VERITAS low and high flux states of $\Gamma_{\rm int,low} \approx 2.5$ and $\Gamma_{\rm int,high} \approx 2.1$, respectively.

X-ray spectral analysis of the *Swift* XRT and *RXTE* PCA data is performed with *XSPEC* 12.4. An absorbed power law model, including the *phabs* model for the photoelectric absorption, is fit to each spectrum. First, a joint fit of the eight *Swift* XRT over the energy range 0.4–10 keV using a tied column density N_H and each spectrum having a varying photon index and normalization is compared to a joint fit with a fixed Galactic column density $N_{H,Gal}$ of $1.50 \cdot 10^{21}$ cm^{-2} (Kalberla et al. 2005). The joint fit with tied N_H yields a best-fit N_H of $(2.06 \pm 0.13) \cdot 10^{21}$ cm^{-2}, with a reduced χ^2 of 1.03 for 203 degrees of freedom (dof) and chance probability for larger chi-squared statistics (null hypothesis) of 37%. The alternative joint fit with the fixed Galactic column density $N_{H,Gal}$ yields a higher reduced χ^2 of 1.13 for 204 dof and null hypothesis of 9.2%. The best-fit N_H is then used in the absorbed power law model for the *RXTE* PCA spectra, which are mostly unaffected by absorption due to the 3–20 keV energy range, and for all *Swift* XRT results presented here. Figure 3 shows *Swift* XRT (0.4–10 keV) and *RXTE* PCA (3–20 keV) spectra from example moderate-flux and high-flux observations. The ratio in each energy bin of the data to the absorbed power law model is shown for the example spectra, with the full list of reduced χ^2 values per dof for each observation listed in Table 1. The model describes well the spectra, yielding an average chance probability for larger chi-squared statistics of 37% and 51% for the *Swift* XRT and *RXTE* PCA data, respectively. The measured *Swift* XRT 0.4–10 keV photon indices range from $\Gamma = 2.33 \pm 0.05$ to $\Gamma = 1.97 \pm 0.05$ for observations differing in 2–10 keV integrated flux by a factor of 6.54 ± 0.52. These results are consistent with the *BeppoSAX* 0.5–10 keV photon indices of $\Gamma \approx 1.8$–2.3 at similar flux levels for an absorbed power law model with fixed Galactic column density (Giommi et al. 2000). Detailed results from the nightly *RXTE* PCA and *Swift* XRT spectra focusing on the connection between the significant X-ray spectral and flux variability are presented in the following section.

6. Light Curves

The nightly VHE γ-ray and X-ray light curve of 1ES 2344+514 from VERITAS, *RXTE* PCA, and *Swift* XRT is shown in Figure 4. A strong VHE γ-ray flare is seen on 2007 December 7 (54441.12 MJD) at an integrated flux F(>300 GeV) $= (6.8 \pm 0.6) \times 10^{-11}$ cm^{-2} s^{-1}, corresponding to 48% of the Crab Nebula flux. The measured increase in flux of a factor of 1.9 ± 0.5 between the previous night and the flare night shows the first clear evidence of ~day time-scale VHE γ-ray variability from 1ES 2344+514 since the Whipple 10 m discovery of VHE γ-ray emission in 1995

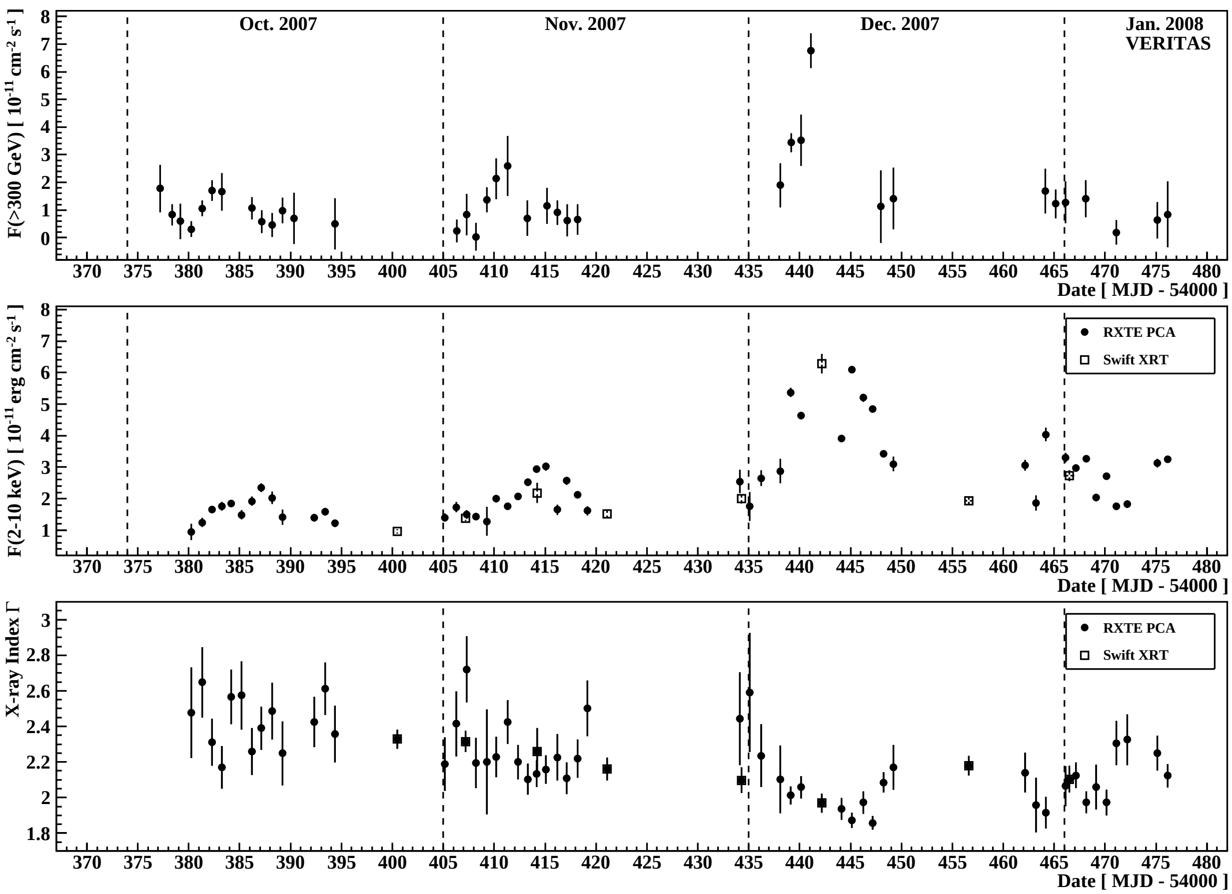

Fig. 4.— VHE γ-ray and X-ray light curve of 1ES 2344+514. Shown in the top panel are VERITAS F(>300 GeV) nightly fluxes. The middle panel shows the 2–10 keV fluxes from observations with *RXTE* PCA (circles) and *Swift* XRT (open squares). The bottom panel shows X-ray photon indices from the best-fit absorbed power law model.

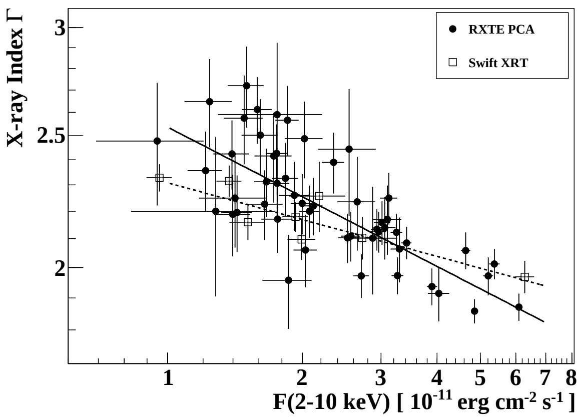

Fig. 5.— X-ray photon index versus 2-10 keV flux from *RXTE* PCA (circles) and *Swift* XRT (open squares) data on a log-log scale. The best-fit power law for the *RXTE* PCA (3–20 keV) data is represented by a solid line, and for *Swift* XRT (0.4–10 keV) with a dashed line.

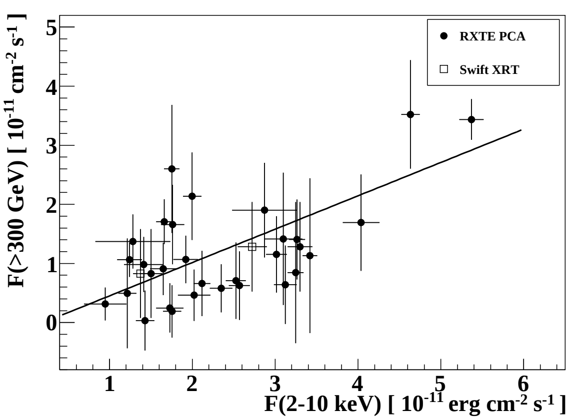

Fig. 6.— VERITAS γ-ray flux F(>300 GeV) versus X-ray 2–10 keV flux from nights with *RXTE* PCA (circles) and *Swift* XRT (open squares) data. A linear fit to the data is represented by the solid line.

(Catanese et al. 1998). Excluding the 2007 December 7 flaring event, the average F(E>300 GeV) is $(1.1 \pm 0.1) \times 10^{-11}$ ph cm^{-2} s^{-1}, corresponding to 7.6% of the Crab Nebula flux. A fit to a constant flux excluding the flaring night is rejected with a chance probability of 7.2×10^{-8}, indicating significant low-level variability. A measure of the integrated level of flux variability is the fractional root-mean-square (rms) variability amplitude $F_{\rm var}$ (Vaughan et al. 2003). For the full VERITAS data set of nightly exposures a high level of variability $F_{\rm var} = (75 \pm 10)\%$ is implied. Excluding the flare night, a still significant $F_{\rm var} = (34 \pm 16)\%$ is determined. Searches for short-term flux variations within each of the nightly observations showed no significant variability.

Figure 4 (lower panels) shows the 2–10 keV flux and photon index Γ measured over 3–20 keV from *RXTE* PCA and 0.4–10 keV from *Swift* XRT data. The X-ray flux is shown to be highly variable throughout the campaign, with $F_{\rm var} = (51 \pm 1)\%$. In 2007 December, large amplitude flaring is evident with flux doubling time-scales of $\sim$1 day. A 2–10 keV flux of $(6.3 \pm 0.3) \times 10^{-11}$ erg cm^{-2} s^{-1} is seen from the Swift XRT data on 2007 December 8, representing the highest X-ray flux ever measured for 1ES 2344+514. Analysis of all subsequent X-ray data of 1ES 2344+514, which currently consists solely of *Swift* XRT observations, show a 2–10 keV flux consistent with the lowest flux measurements presented here. Detailed results from the more recent *Swift* XRT data set are beyond the scope of this publication, but automated count rate light curves are publicly available.[2]

X-ray spectral variability between flaring nights is investigated by plotting the X-ray photon index Γ versus the 2–10 keV flux, shown in Figure 5. A logarithmic correlation of decreasing photon index with increasing flux is suggested from a power law fit to the *RXTE* PCA and *Swift* XRT data with a χ^2/dof probability of 0.14 and 0.70 compared to 7.9 $\times 10^{-20}$ and 3.3 $\times 10^{-4}$ for a constant photon index, respectively. Due to the lack of significant curvature in the X-ray spectrum, the peak energy E_p for a $\nu F(\nu)$ SED representation is

[2]The *Swift* XRT Monitoring of *Fermi* LAT Sources of Interest is available online at: http://www.swift.psu.edu/monitoring/

largely unconstrained. A comparison of the photon indices from the *Swift* XRT and *RXTE* PCA spectra restricted to the overlapping energy range of 3–10 keV is limited by the low number of energy bins above 3 keV, so a study of the systematically higher *RXTE* PCA (3–20 keV) photon indices compared with the *Swift* XRT (0.4–10 keV) photon indices at similar flux levels is inconclusive. Furthermore, the lack of purely simultaneous *RXTE* PCA and *Swift* XRT data does not allow for a detailed study of joint fits from 0.4–20 keV. Even during the bright flaring events in 2007 December, the *RXTE* PCA spectra from 3–20 keV show no sign of curvature, with measured photon indices of $\sim$1.9. For these high-flux states the implied peak energy $E_p \leq 10$ keV agrees with the estimated peak energies derived from *BeppoSAX* observations in 1998 (Giommi et al. 2000).

Figure 6 shows the VERITAS flux F(>300 GeV) versus *RXTE* PCA and *Swift* XRT 2–10 keV fluxes for nights with observations in both energy bands. A Pearson coefficient of $r = 0.60 \pm 0.11$ is calculated for the VHE γ-ray to X-ray flux points, suggestive of correlated variability. The best-fit linear model yields a slope of 0.56 ± 0.08 with a fit probability of 0.14. For the highest measured X-ray fluxes in 2007 December the weather conditions at the VERITAS site were poor, which excludes these nightly fluxes from figure 6. Due to the sparse data sampling, a search for lags between the VHE γ-ray and X-ray emission is not investigated here.

7. Discussion

The broadband spectral energy distribution (SED) of high-frequency-peaked BL Lac objects (HBLs) is often modeled within a synchrotron self-Compton (SSC) framework. Simple one-zone SSC models typically predict correlated X-ray and VHE γ-ray variability from the underlying electron distribution. Figure 7 shows a one-zone SSC model calculation (Krawczynski et al. 2004) to the SED of 1ES 2344+514 for illustration purposes in two flux states. A high flux SED is constructed from the VERITAS photon spectrum in 2007 December 7 and *Swift* UVOT and XRT data on 2007 December 8. The time-averaged (flare excluded) VERITAS data is combined with *Swift* and *RXTE* PCA spectra on 2008 January 1 when the object was at a moderate X-ray flux state with respect to the full campaign. Shown also in Figure 7 are the non-contemporaneous MAGIC data from 2005 in a low flux state and the flaring Whipple 10 m data from 1995 December 20. Also shown for reference is the *Fermi* LAT spectrum from 2008 August to 2009 July in a non-variable low flux state. Each model curve for the broadband data contemporaneous with the VERITAS data represents the intrinsic source radiation, and all VHE γ-ray spectra are corrected for absorption by the extragalactic background light (Franceschini et al. 2008). The SSC model input parameters for the low (high, when different) states are: a Doppler factor $\delta = 13$ (20), magnetic field = 0.09 G (0.03 G), emission radius = 10^{16} cm, electron density = 0.05 ergs cm^{-3}, and a broken power law electron spectrum with low-energies between 10^8 eV and $10^{11.3}$ eV ($10^{11.4}$ eV) with spectral index $n_1 = 2.5$ (2.3), and above the cutoff energy with index $n_1 = 3.2$ and highest energy of 10^{12} eV.

The light crossing time $\tau = R/(c \times \delta) \approx 5$ hours for the high flux state with a Doppler factor $\delta = 20$ is consistent with the $\sim$hour time-scale X-ray variability seen from 1ES 2344+514 with *BeppoSAX* on 1996 December 7 (Giommi et al. 2000). Further hourly X-ray variability in 1ES 2344+514 could not be confirmed in this work due to the short (<hour) exposures with *Swift* and *RXTE* and moderate event statistics. In addition to the low and high flux state modeling from data in 2007 October to 2008 January, the same SSC model was applied to non-contemporaneous low and high flux states derived from *BeppoSAX*, MAGIC, and Whipple 10 m spectra (Albert et al. 2007). A reasonable agreement between model parameters, such as Doppler factors $\sim$10–20 and a magnetic field $\sim$0.03–0.3 G, is evident for both the low and high flux states with the archival 1ES 2344+514 data, and compared with one-zone SSC modeling of similar moderate-flux level flares in the HBLs 1ES 1959+650 (Tagliaferri et al. 2008), 1ES 0806+524 (Acciari et al. 2009), and 1ES 1101-213 (Aharonian et al. 2007). A detailed study of the SSC model parameter space (e.g. (Tavecchio, Maraschi & Ghisellini 1998)) is not pursued here due to sparseness in the SED coverage and degeneracy between model parameters. The simple one-zone SSC modeling presented here adequately describes the data, however fur-

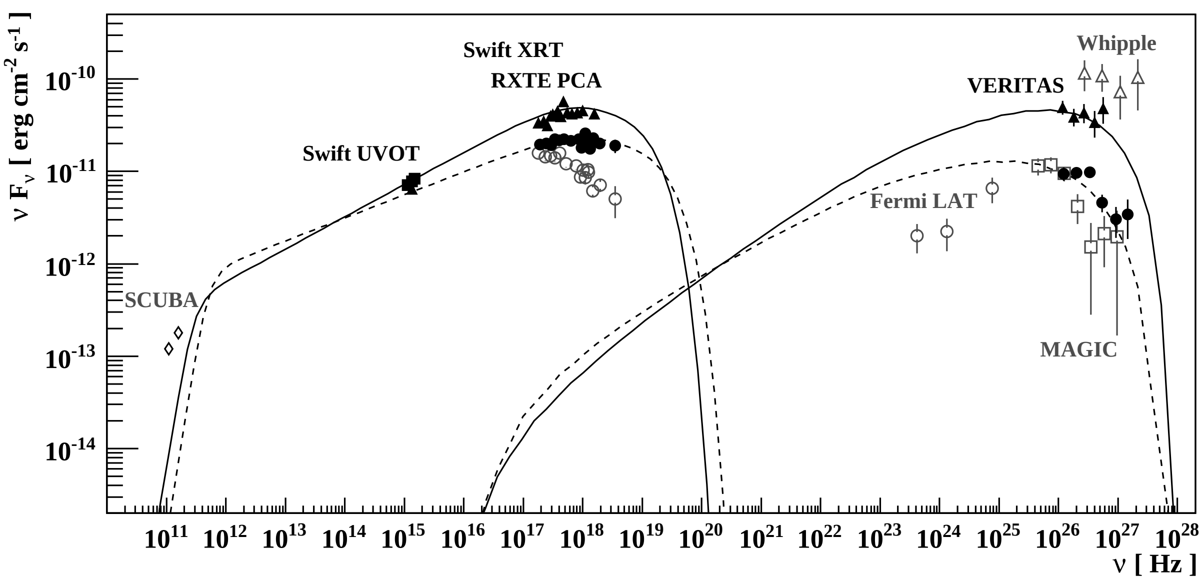

Fig. 7.— Spectral energy distribution of 1ES 2344+514. The high flux spectrum (triangles) are from VERITAS data on 2007 December 7 and *Swift* UVOT and XRT data on 2007 December 8. The time-averaged VERITAS spectrum and moderate flux level X-ray spectrum from *Swift* XRT and *RXTE* PCA data on 2008 January 1 are represented by circles. An example low flux X-ray spectrum (open circles) is from 2007 November 3. Non-contemporaneous VHE γ-ray spectra are shown from MAGIC data in 2005 August–December (open squares) and from Whipple 10 m data on the flare night of 1995 December 20 (open triangles). All VHE γ-ray spectra are corrected for absorption by the extragalactic background light (Franceschini et al. 2008). Archival millimeter fluxes (open diamonds) are from SCUBA data (Stevens & Gear 1999). The non-contemporaneous *Fermi* LAT spectrum from the 1FGL catalog is represented by open circles (Abdo et al. 2010). The broadband curves are from synchrotron self-Compton (SSC) modeling to the contemporaneous data (Krawczynski et al. 2004).

ther optical, X-ray, and VHE γ-ray observations of 1ES 2344+514 simultaneous with *Fermi* LAT promise to offer stronger constraints to emission models.

8. Conclusion

In this paper, a $\sim$4 month long VHE γ-ray and X-ray observing campaign of 1ES 2344+514 revealed significant flux variability on $\sim$1 day timescales. In particular, flux doubling between nights is evident in both the X-ray and VHE γ-ray bands in 2007 December, with the highest ever X-ray flux measured from 1ES 2344+514 on 2007 December 8. Evidence of correlated nightly X-ray flux and VHE γ-ray flux variability is shown, as generally found in the well-studied HBLs Mrk 501 (Krawczynski et al. 2000), Mrk 421 (Fossati et al. 2008), and 1ES 1959+650 (Krawczynski et al. 2004), however so-called orphan flares of increased flux in one energy band and not the other have also been observed (e.g. (Błażejowski et al. 2005; Krawczynski et al. 2004)). For these campaigns sparse temporal sampling and insufficient VHE sensitivity to short time-scale variability limited any statements on a linear or quadratic relationship between VHE and X-ray flux expected under various SSC scenarios during rising or decaying flares (Fossati et al. 2008). The 1ES 2344+514 data presented here represents the first contemporaneous multiwavelength campaign of the object from UV to VHE γ-rays, but is similarly restricted by sparse temporal sampling and broadband coverage in the spectral energy distributions. Applying a simple one-zone SSC model reasonably describes the data, and is consistent with past modeling of the object and other HBLs. Further optical, X-ray, and VHE γ-ray observations of 1ES 2344+514 simultaneous with *Fermi* LAT in the HE γ-ray band promise to offer stronger constraints to emission models and high sensitivity broadband measurements of high-flux state flaring events.

This research is supported by grants from the U.S. Department of Energy, the U.S. National Science Foundation, and the Smithsonian Institution, by NSERC in Canada, by STFC in the UK and by Science Foundation Ireland. Special acknowledgment to the Swift and RXTE teams for the support of these observations.

REFERENCES

Abdo, A. A., et al. 2010, ApJS, 2010, 188, 405

Acciari, V. A., et al. 2008, ApJ, 679, 1427

Acciari, V. A., et al. 2009, ApJ, 690, L126

Albert, J., et al. 2007, ApJ, 662, 892

Aharonian, F. 2000, New Astron., 5, 37

Aharonian, F., et al 2001, A&A, 370, 112

Aharonian, F., et al. 2004, A&A, 421, 529

Aharonian, F., et al. 2007, A&A, 470, 475

Blandford, R. D., & Königl, A. 1979, ApJ, 232, 34

Błażejowski, M., et al. 2005, ApJ, 630, 130

Böttcher, M. & Chang, J. 2002, ApJ, 581, 127

Bradt, H. V., Rothschild, R. E., & Swank, J. H. 1993, A&AS, 97, 355

Burrows, D., et al. 2005, SSRv., 120, 165

Catanese, M., et al. 1998, ApJ, 501, 616

Coppi, P. S. 1992, MNRAS, 258, 657

Daniel, M. K., et al. 2007, Proc. 30th ICRC, Merida, Mexico, 283

Dickey, J. M. & Lockman, F. J. 1990, ARA&A, 28, 215

Elvis, M., et al. 1992, ApJS, 80, 257

Falomo, R. & Kotilainen, J. K. 1999, A&A, 352, 85

Fitzpatrick, E., PASP, 111, 63

Fossati, G., et al. 2008, ApJ, 677, 906

Franceschini, A., et al. 2008, A&A, 487, 837

Gehrels, N., et al. 2004, ApJ, 611, 1005

Giommi, P., Padovani, P. & Perlman, E. 2000, MNRAS, 317, 743

Giroletti, M. et al. 2004, ApJ, 613, 752

Godambe S. V., et al. 2007, J. Phys. G: Nucl. Part. Phys., 34, 1683

Gould, R. J. & Schréder, G. P. 1967, Phys. Rev., 155, 1408

Gupta, A. C., et al. 2008, AJ, 135, 1384

Hillas A. M., 1985, Proc. 19th ICRC, La Jolla, USA, 3, 445

Hofmann, W., et al. 1999, Astropart. Phys., 12, 135

Holder, J., et al. 2006, Astropart. Phys., 25, 361

Johoda, K., et al. 1996, SPIE, 2808, 59

Kalberla, P. M. W., et al. 2005, A&A, 440, 775

Krawczynski, H., et al. 2000, A&A, 353, 97

Krawczynski, H., et al. 2004, ApJ, 601, 151

Krawczynski, H., et al. 2006, Astropart. Phys., 25, 380

Mannheim, K. 1993, A&A, 269, 67

Mücke, A. & Protheroe, R. J. 2001, Astropart. Phys., 15, 121

Nilsson, K., et al. 1999, PASP, 111, 1223

Perlman, E. S., et al. 1996, ApJS, 104, 251

Poole, T. S., et al. 2008, MNRAS, 383, 627

Rector, T. A., Gabuzda, D. C. & Stocke, J. T. 2003, AJ, 125, 1060

Schroedter, M., et al. 2005, ApJ, 634, 947

Stevens, J. A. & Gear, W. K. 1999, MNRAS, 307, 403

Tagliaferri, G., et al. 2008, ApJ, 679, 1029

Tavecchio, F., Maraschi, L., & Ghisellini, G. 1998, ApJ, 509, 608

Tramacere, A., et al. 2007, A&A, 467, 501

Vaughan, S. et al. 2003, MNRAS, 345, 1271

Weekes, T. C., et al. 2002, Astropart. Phys., 17, 221

Xie, G. Z., et al. 2002, MNRAS, 329, 689

This 2-column preprint was prepared with the AAS LaTeX macros v5.2.